Journal of Visualized Experiments

Experimental Approach for Determining Semiconductor/liquid Junction Energetics by Operando Ambient-Pressure X-ray Photoelectron Spectroscopy

--Manuscript Draft--

Manuscript Number:	JoVE54129R3
Full Title:	Experimental Approach for Determining Semiconductor/liquid Junction Energetics by Operando Ambient-Pressure X-ray Photoelectron Spectroscopy
Article Type:	Methods Article - JoVE Produced Video
Keywords:	Artificial Photosynthesis; Renewable Energy; Semiconductors; photovoltaics; Interfaces; Corrosion Protection
Manuscript Classifications:	5.7.305.625: Semiconductors; 92.23.7: spectroscopic analysis (chemistry); 92.24.29: testing of materials (composite materials); 97.76.25: semiconductor materials
Corresponding Author:	Michael Frankston Lichterman California Institute of Technology Pasadena, California UNITED STATES
Corresponding Author Secondary Information:	
Corresponding Author E-Mail:	mlichter@caltech.edu
Corresponding Author's Institution:	California Institute of Technology
Corresponding Author's Secondary Institution:	
First Author:	Michael Frankston Lichterman
First Author Secondary Information:	
Other Authors:	Matthias H Richter
	Shu Hu
	Ethan J Crumlin
	Stephanus Axnanda
	Marco Favaro
	Walter Drisdell
	Zahid Hussein
	Bruce S Brunschwig
	Nathan S Lewis
	Zhi Liu
	Hans-Joachim Lewerenz
Order of Authors Secondary Information:	
Abstract:	Operando Ambient Pressure X-ray photoelectron spectroscopy (operando AP-XPS) investigation of semiconductor/liquid junctions provides quantitative understanding of the energy bands in these photoelectrochemical solar cells. Liquid junction photoelectrochemical cells allow a uniform contact between the light-absorbing semiconductor and its contacting aqueous electrolyte phase. Standard Ultra High

Powered by Editorial Manager® and ProduXion Manager® from Aries Systems Corporation

	Vacuum (UHV) based X-ray photoelectron spectroscopy (XPS) has been used to analyze the electronic energy band relations in solid-state photovoltaics. We demonstrate how operando AP-XPS may be used to determine these relationships for semiconductor/liquid systems. The use of "tender" X-ray synchrotron radiation produces photoelectrons with enough energy to escape through a thin electrolyte overlayer; these photoelectrons provide information regarding the chemical and electronic nature of the top ~10 nm of the electrode as well as of the electrolyte. The data can be analyzed to determine the energy relationship between the electronic energy bands in the semiconductor electrode and the redox levels in the solution. These relationships are critical to the operation of the photoelectrochemical cell and for understanding such processes as photoelectrode corrosion or passivation. Through the approach described herein, the major conditions for semiconductor-electrolyte contacts including accumulation, depletion, and Fermi-level pinning are observed, and the so-called flat-band energy can be determined.
Author Comments:	This manuscript was invited by Alison Hamlin.
Additional Information:	
Question	**Response**
If this article needs to be "in-press" by a certain date to satisfy grant requirements, please indicate the date below and explain in your cover letter.	

Manuscript Click here to download Manuscript 54129_R3_RE.docx

TITLE:
Experimental Approach for Determining Semiconductor/liquid Junction Energetics by *Operando* Ambient-Pressure X-ray Photoelectron Spectroscopy

AUTHORS:
*Lichterman, Michael F.
Division of Chemistry and Chemical Engineering
California Institute of Technology
Pasadena, CA, USA
mlichter@caltech.edu

*Richter, Matthias H.
Joint Center for Artificial Photosynthesis
California Institute of Technology
Pasadena, CA, USA
mrichter@caltech.edu

*Hu, Shu
Division of Chemistry and Chemical Engineering
California Institute of Technology
Pasadena, CA, USA
shuhu@caltech.edu

*Crumlin, Ethan J.
Advanced Light Source
Lawrence Berkeley National Laboratory
Berkeley, CA, USA
ejcrumlin@lbl.gov

Axnanda, Stephanus
Advanced Light Source
Lawrence Berkeley National Laboratory
Berkeley, CA, USA
saxnanda@lbl.gov

Favaro, Marco
Advanced Light Source
Lawrence Berkeley National Laboratory
Berkeley, CA, USA
mfavaro@lbl.gov

Drisdell, Walter
Advanced Light Source
Lawrence Berkeley National Laboratory
Berkeley, CA, USA
wsdrisdell@lbl.gov

Hussain, Zahid
Advanced Light Source
Lawrence Berkeley National Laboratory
Berkeley, CA, USA
zhussain@lbl.gov

Brunschwig, Bruce S.
Beckman Institute
California Institute of Technology
Pasadena, CA, USA
bsb@caltech.edu

Lewis, Nathan S.
Division of Chemistry and Chemical Engineering
California Institute of Technology
Pasadena, CA, USA
nslewis@caltech.edu

Liu, Zhi
Advanced Light Source
Lawrence Berkeley National Laboratory
Berkeley, CA, USA
Zliu2@lbl.gov

Lewerenz, Hans-Joachim
Joint Center for Artificial Photosynthesis
California Institute of Technology
Pasadena, CA, USA
lewerenz@caltech.edu

*: These authors contributed equally to this work.

CORRESPONDING AUTHOR:
Lewerenz, Hans-Joachim

KEYWORDS:
Artificial Photosynthesis, Renewable Energy, Semiconductors, Photovoltaics, Interfaces, Corrosion Protection

SHORT ABSTRACT:
We present a method for the determination of the energy relations of semiconductor/liquid junctions, which are the basis for the successful operation of such renewable solar energy converting systems.

LONG ABSTRACT:

Operando Ambient Pressure X-ray photoelectron spectroscopy (*operando* AP-XPS) investigation of semiconductor/liquid junctions provides quantitative understanding of the energy bands in these photoelectrochemical solar cells. Liquid junction photoelectrochemical cells allow a uniform contact between the light-absorbing semiconductor and its contacting electrolyte phase. Standard Ultra High Vacuum (UHV) based X-ray photoelectron spectroscopy (XPS) has been used to analyze the electronic energy band relations in solid-state photovoltaics. We demonstrate how *operando* AP-XPS may be used to determine these relationships for semiconductor/liquid systems. The use of "tender" X-ray synchrotron radiation produces photoelectrons with enough energy to escape through a thin electrolyte overlayer; these photoelectrons provide information regarding the chemical and electronic nature of the top ~10 nm of the electrode as well as of the electrolyte. The data can be analyzed to determine the energy relationship between the electronic energy bands in the semiconductor electrode and the redox levels in the solution. These relationships are critical to the operation of the photoelectrochemical cell and for understanding such processes as photoelectrode corrosion or passivation. Through the approach described herein, the major conditions for semiconductor-electrolyte contacts including accumulation, depletion, and Fermi-level pinning are observed, and the so-called flat-band energy can be determined.

INTRODUCTION:

Semiconductor/liquid junctions have long been investigated due to their simplicity of construction and economical possibility of fuel generation [1-4], with some such systems obtaining efficiencies over 17%.[5] These systems operate based on the formation of a rectifying junction at the interface between the semiconductor electrode and the electrolyte. The energetics of semiconductor/liquid junctions are similar to those of a semiconductor/metal, Schottky, junction [3] where an electrolyte assumes the role of the metal. The semiconductor Fermi level, E_F, is the electrochemical potential of the electron in the semiconductor and is analogous to the chemical potential of an electron in solution. In a liquid junction cell the difference in the chemical potential of the electron between the two phases results in the transfer of charge from one phase to another at equilibrium. Since the ions in the electrolyte are free to move while the fixed charges in the semiconductor cannot, a space-charge (or depletion) region forms within the semiconductor with an accompanying electric field. This electric field shifts the Fermi level (electrochemical potential) of the semiconductor to be equal to the chemical potential of the electron in the solution [6]. The resulting electric field in the semiconductor only exists close (~ 1 μm) to the solution interface and the energy of the electron levels in this region are viewed as being "bent" by the field. The "band bending" in the semiconductor space-charge region results in a barrier to current flow in one direction while allowing conduction in the opposite direction, producing a "rectifying junction". Under illumination, this electrical field in the near-surface region of the semiconductor can separate light-generated electrons and holes, such that the device can be operated in a manner analogous to a solid-state photovoltaic device. Figure 1 demonstrates these basic concepts.

[Place Figure 1 here]

X-ray photoelectron spectroscopy (XPS) is a widely-used technique for determining both chemical (i.e., oxidation) states and electronic effects such as energy band relations in solid materials. Because of the very small inelastic mean free path (IMFP) of photoelectrons in air,

including IMFPs on the mm scale even at millibar pressures[7], and in order to avoid changes of the probed surfaces during measurements, XPS generally has to be performed under ultra-high vacuum (UHV) conditions. Numerous reviews of the XPS technique have been written [8-10]. In XPS, typically, electrons from core levels of the constituent elements of the sample are ejected into the vacuum by the absorption of X-rays. Upon irradiation with X-rays of an energy *hν*, electrons are ejected from the sample having a kinetic energy E_{Kvac} with respect to the vacuum level $E_{VAC.}$ Figure 2 shows (a) the general geometry of an XPS instrument, (b) a simulated XPS spectra of TiO_2 with core levels (CL), Auger lines and a measurement of the work function, and (c) the relation of photon energy to kinetic and binding energies. The conservation of energy requires

$$h\nu = E_B + E_{Kvac} + \phi \qquad (1)$$

where E_B is the binding energy of the photoelectron from the core level, and ϕ is the work function of the sample. E_B is referenced to the Fermi level of the sample, E_F. The position of E_F can be determined by measurement of the valence band maximum of a noble metal (i.e. Gold or Silver) and fitting the Fermi function when the photon energy is well known (i.e. Al Kα). Otherwise this procedure is used to calibrate the photon energy, i.e. at electron synchrotrons that produce X-rays of variable energy.

[Place Figure 2 here]

Recently, ambient-pressure XPS, AP-XPS, experiments have been made possible due to the construction of differentially pumped electrostatic lens equipped ambient-pressure XPS analyzer systems. One approach to doing XPS at a solid/liquid interface is to separate the vacuum and the solution with a thin membrane through which XPS is carried out[11-13]. This technique requires the use of extremely thin membranes of materials such as silicon or graphene, as opposed to allowing measurements on thicker semiconductor materials. While standard XPS is carried out under UHV (10^{-9} – 10^{-11} Torr), in AP-XPS the sample is at tens of Torr pressure while the analyzer remains under HV/UHV conditions. The resulting large pressure difference is realized by multiple stages of differential pumping [7,14]. As a result, measurement conditions much closer to a normal working environment can be realized. Studies on gold oxidation [15], lithium-oxygen redox reactions [16], and catalytic reactions [17] have been carried out in such systems. Further development and refinement of the technique [18] has allowed use of an electrochemical cell as the sample with the ability to apply a potential difference between the working electrode and the solution in a three-electrode electrochemical cell, which we term *operando* AP-XPS. The surface of the working electrode under a thin meniscus of electrolyte is analyzed by the *operando* AP-XPS technique. Figure 3 shows (a) a general schematic of the endstation as well as (b-d) pictures of the various parts of the endstation and (e) the materials under investigation. As a result, the solid working electrode as well as the thin (~13 nm) electrolyte layer can be investigated simultaneously, provided that the photoelectrons have a sufficient kinetic energy to penetrate through the electrolyte overlayer and escape unscattered, i.e. without energy loss, to the analyzer/detector. The use of ~ 4 keV X-rays produces photoelectrons with sufficient kinetic energy (~3.5 keV for Ti 2p and O 1s core levels) to make this possible [18].

[Place Figure 3 here]

We have recently demonstrated that the combination of atomic-layer deposition (ALD)-grown

TiO_2 with a Ni catalyst can effectively stabilize a variety of semiconductors in alkaline media, including Si, GaP, GaAs [19], CdTe [20], and $BiVO_4$ [21] against photocorrosion. This advancement enables the use of technologically advanced semiconductors for energy converting devices such as solar fuel generators. Further investigation of the working principles of TiO_2 in these systems was undertaken to evaluate the nature of the semiconductor/liquid junction in the presence or absence of Ni [22-24]. Direct observation of these junctions using the *operando* AP-XPS approach produces data which demonstrate the working principles (accumulation, Fermi level pinning, depletion, inversion) behind these systems. Furthermore, this approach provides a tool by which a semiconductor/liquid junction or photocatalyst[25,26] may be interrogated such that the fundamental operating characteristics may be understood and optimized. We describe herein the manner in which such investigations may be undertaken, the conditions that are required for these experiments to work, and the means by which the data collected may be understood. We describe, in sections 1-2, the preparation of the electrodes which were used in our experiments, before presenting more general directions (sections 3-5) regarding the collection of data using this approach.

PROTOCOL:

1. Preparation of Semiconductor for Analysis

1.1) Clean a p^+, (100)-oriented boron doped Czochralski-grown Si wafer with a resistivity of $\rho < 0.005\ \Omega\cdot cm$. First soak for 2 min in a 3:1 (by volume) "piranha" solution of concentrated H_2SO_4 (98%) to 30% $H_2O_{2(aq)}$.

1.2) Etch for 10 s in a 10% (by volume) solution of $HF_{(aq)}$.

1.3) Immediately after step 1.2, etch in a 5:1:1 (by volume) solution of H_2O, 36% hydrochloric acid, and 30% hydrogen peroxide for 10 min at 75 °C before moving the sample into the ALD chamber.

1.4) Deposit the TiO_2 from a tetrakis(dimethylamido)titanium (IV) (TDMAT) precursor in an ALD reactor. Set the sample temperature to 150 °C.

1.5) Carry out the deposition beginning with a pulse of TDMAT for 0.1 s, followed by a purge for 15 s with N_2 at 20 sccm (with constant N_2 flow/purge over the complete deposition period).

1.6) Proceed with a 0.015 s pulse of H_2O before another 15 s purge with N_2. This completes one full ALD cycle. Repeat this process (1.4-1.5) for 1500 cycles to provide films ~ 70 nm in thickness.

1.7) Where desired, deposit Ni at a rate of ~ 2 nm per min by use of a RF sputtering power of 150 W for 20 s – 300 s in a sputtering system. Use Ar as the sputtering gas at a pressure of approximately 8.5 milliTorr.

[Place Figure 4 here]

2. Construction of Electrodes for the Endstation

2.1) Cut strips of the semiconductor sample into rectangles approximately 1 cm x 3.5 cm in size.

2.2) Using a scribe, scratch In/Ga eutectic into the back of the Si wafer to create an ohmic contact to the Si.

2.3) Cut pieces of 1 mm thick glass to approximately 0.8 cm x 4 cm in size as the support. Add 1-sided copper tape to the glass to cover it, with the sticky side of the copper tape on the glass as the back contact.

2.4) Add silver paint to the copper tape on the glass support and the back of the Si wafer. Push the back of the Si wafer to the copper tape on the glass support and let dry.

2.5) Use epoxy (stable in 1 M KOH) to encapsulate the edges and back of the sample such that only the front of the TiO_2/Si sample can be contacted by solution.

2.6) For the counter electrode, use a Pt or Ni foil.

3. Preparation of Electrolyte(s) and Materials for Beamline Experiments

3.1) Prepare (or purchase) all necessary electrolytes. For 1.0 M KOH, add 56 g of KOH (semiconductor grade, 99.99%) to 1.0 L of water (18.2 MΩ cm at 25 °C resistivity) and let cool.

3.2) Use a pH meter to measure the pH of the resulting solution, and add KOH pellets or H_2O until true pH 14 solution is prepared.

3.3) Add excess electrolyte (100 mL) to a clean beaker and place under vacuum to degas the solution. Also prepare a beaker of pure water (18.2 MΩ cm at 25 °C resistivity), degassed in a similar manner. A properly degassed electrolyte will remain at a constant vapor pressure under static vacuum.

3.4) Clean the beaker that will be used to hold the electrolyte by immersing in aqua regia. Prepare aqua regia by adding 1 part (15 mL) nitric acid (concentrated) to 3 parts (45 mL) 36% hydrochloric acid. Clean the beaker by washing with copious amounts of water (18.2 MΩ cm at 25 °C resistivity).

4. Photoelectron Spectroscopy Energy Calibration

4.1) Mount a gold foil onto the sample holder arm in the working electrode slot, and test contact to the arm with a multimeter.

4.2) Insert the sample holder arm into the endstation with a copper gasket between the endstation and sampler holder arm flange. Attach the sample holder arm to the endstation through a copper gasket.

4.3) Open valve to vacuum for the sample chamber to pull vacuum on this chamber. Once pressure has decreased below 20 Torr, open the analyzer cone by removing the wobble stick.

4.4) Lower the sample using z-axis controls into sampling height. Turn on the detector; focus sample in x- and y- axes by measuring count rate for Au 4f photoelectrons; a maximum (ideally > 200,000 counts per second) indicates a focused spot.

4.5) Collect XPS data (by selecting the appropriate core level and starting the scan from within the software) for the Au 4f core level, and record the peak positions. Calibrated binding energy for the metallic Au $4f^{7/2}$ core level is 84.0 eV. For a more detailed description please see section 5.6.

4.6) Collect XPS data for the Au Fermi edge (near zero binding energy). Use as a secondary calibration if necessary.

4.7) Turn off the detector; back the sample away from the detector cone and raise the sample before placing wobble stick on the detector cone to isolate the detector. Flood the chamber with N_2 to remove the vacuum. Remove the sample holder arm.

5. Photoemission Measurement and Data collection

5.1) Mount working electrode (semiconductor sample), a Pt foil counter electrode, and a leakless Ag/AgCl reference electrode, to the sample holder arm. Mount the working electrode to face the collection cone. Rinse with water to ensure removal of any KCl or dust. Ensure that the liquid nitrogen in the vacuum traps (which condenses evaporated electrolyte) is full, and once full, refill within every 2 hours.

5.2) Attach sample holder arm to the endstation. Place the electrolyte beaker on the beaker holder platform and fill with degassed electrolyte; place degassed water beaker inside chamber as well (as a sacrificial electrolyte). Ground the working electrode metallic outside contact on the sample holder arm to the instrument; attach the working, counter, and reference electrode leads to their respective leads from the potentiostat.

5.3) Slowly open the valve to apply vacuum until a stable vacuum near 15 Torr is reached.

5.4) Remove wobble stick and lower the electrodes into the beaker (z-axis) (Figure 5a), without approaching the detector cone (x-axis). Record the height of the detector cone opening, as well as the height of the top of the electrolyte, in terms of the z-axis position.

5.4.1) If necessary, take preliminary cyclic voltammogram (CV) measurements or undertake oxidation reactions to ensure a hydrophilic surface. Ensure that the potentials under which the experiment will be run do not cause substantial bubbles to approach the detector cone.[27]

5.5) Based on the CV data, choose an initial potential and set this potential. Turn on the detector. Retract by approximately the difference in height between the cone opening and the electrolyte surface level and focus in the x and y positions (Figure 5b) by analyzing the count rate of the

sample material, *not* the O 1s count rate. Collect sample and water XPS data and adjust x, y, and z values until a spot is found which contains both liquid water, near 536 eV binding energy, and the sample core levels (here, Ti 2p and Ni 2p) in the XPS data.

Note: Preferably, choose a potential range in which the hydrophilic nature of the electrode surface can be maintained based on the CV data that will produce X-ray data which will provide information about the electrochemical nature of the system.

5.6) Collect all necessary XPS data at this potential (Figure 5c), including sample core levels such as Ti 2p and Ni 2p, as well as O 1s data, by selecting these core level areas within the detection software and performing data collection.

5.6.1) Generally, open the scan selection window within the software by selecting "setup" from the "run" pull-down menu. On the setup page, select a scan and click "edit" to to modify the energy parameters of the scan. Alternateively, enter a new scan profile, by selecting "new,". Select a "check mark" next to a scan to select the scan to be carried out, and click "start" to start the acquisition.

5.6.2) Scan until a sufficient signal-to-noise ratio is observed in the data; this may take between 15 min and multiple hours.

5.7) Retract the sample, in the x-axis, from the detector cone. Lower the sample by the aforementioned electrolyte-cone vertical distance and set a new potential; then, retract by the same distance, focus, and repeat the XPS data collection procedure as described in 5.5-5.6.

5.8) When data collection is complete, turn off the detector, retract the sample in the x and z directions and place the wobble stick onto the detector cone. Flood the chamber with N_2 to bring the chamber back to atmospheric pressure and remove the sample holder arm; remove the electrodes from the arm and the liquids from the sampling chamber.

[Place Figure 5 here]

REPRESENTATIVE RESULTS:

Representative results are shown in Figures 6, 7, and 8. Figure 6 shows the collected O 1s and Ti 2p core level spectra for a TiO_2 electrolyte in 1.0 M KOH solution, stacked with respect to the applied potential. Figure 7 shows the plotted core level water O 1s and Ti 2p peak positions, as collected from Figure 6 as well as from data in which a TiO_2/Ni/electrolyte sample was investigated in the same electrolyte. Figure 8 shows a brief summary of our conclusions from this investigation regarding the nature of the semiconductor/liquid contact.

First, we consider the binding energies of the solid at a semiconductor/liquid or metal/liquid junction. The binding energies for the electrode are measured at the surface of the electrode. For an ideal semiconductor/liquid junction, provided that the space-charge region is significantly thicker than the sampling depth, only the energy bands at the top/edge of the space charge region are probed, i.e. the binding energies are more representative of the interface/surface of the semiconductor than of its bulk properties. In the ideal case, the energy of the band edges (i.e. the

energy of the bands at the solution interface) of the semiconductor are fixed with respect to the solution (no potential drop in the electrolyte); as a result, if the Fermi level is moved to a relatively more positive potential by applying a positive potential to the n-type working electrode, the energy difference between the core levels at the semiconductor/electrolyte interface and the Fermi level will decrease accordingly (formation of a depletion layer in the semiconductor at the surface). Thus the binding energy of the semiconductor core levels will change with the applied voltage with a slope of -1 eV V^{-1} at the semiconductor surface.

For a metal/liquid junction, no band bending can occur since a metal cannot support an electric field within its bulk. Static electric fields are screened within less than an atomic layer by the free electrons of the metal. When a potential is applied across a metal/solution interface, a charge builds up on the surface of the metal that is compensated by an equal and opposite charge in a thin layer of the solution (~1 nm for electrolyte concentration ~1 M). The two layers of charge are known as the electrochemical double layer. This produces an electric field within the double layer, also called the Helmholtz or Stern layer, with the potential solely changing in this region which is about 1 nm thick. This causes the metal energy bands to shift in unison relative to the solution, i.e. the difference between the core level binding energy of the metal to the Fermi level stays constant. Thus the binding energies observed for a metal stay fixed when the applied potential is changed (the slope is now 0 eV V^{-1}), as long as no chemical changes (such as oxidation) occur. For a non-ideal semiconductor junction, the presence of surface defects or chemical interactions with the ambient can result in surface states with a high density of states and an accordingly increased capacitance compared to that of the semiconductor space charge region. This can induce a behavior similar to that of a metal, such that the band edges can shift relative to the solution. In this case, when a potential is applied to the working electrode, the semiconductor bands shift (instead of band bending) and the binding energy does not show a shift with the applied voltage; as a result, the relation of 0 eV V^{-1} is once again observed. Typical conditions for such band edge shifting are strong accumulation or strong inversion in which the semiconductor is biased negative or positive enough of its flat-band potential for n-type so the Fermi level approaches the conduction band or valence band edges with their high density of states. Band edge shifting can also result from Fermi level pinning at (high density) surface states.

The situation for the binding energies of the bulk water is different. They are measured primarily at the surface of the electrolyte (away from the electrode). When the solution consists of a concentrated electrolyte (> 0.1 M), static electrical fields only exist in the electrochemical double layer; beyond that region, the electrolyte is neutral and the binding energy of the O 1s core level of the bulk water (measured predominantly outside the double layer) is expected to shift with applied potential with a slope of -1 eV V^{-1}, analogous to the ideal semiconductor/liquid band edge shifts as the Fermi level is moved positive with respect to the water core levels, i.e., a positive potential is applied to the working electrode.

The peaks in Figure 6a have been fitted, and their relative peak positions are plotted in Figure 7a. Four different regions of applied potential were defined, based on the observed shifts in binding energy for the TiO_2/liquid junction sample. We deduced that in regions with no shift in binding energy for the TiO_2, band edge movement occurs; this can occur due to strong semiconductor accumulation where the Fermi level approaches the conduction band of TiO_2 at very negative

potentials (region U_1) or Fermi level pinning [28] at potential regions where mid-gap defect states occur (region U_3). In other regions, such as U_2 and U_4, the binding energy-potential relationship appears effectively ideal and approaches the -1 eV V^{-1} shift expected. In these regions we conclude that the semiconductor band edges are fixed.

[Place Figure 6 here]

The addition of Ni (by 60 s of sputtering) to the surface of the electrode (Figure 7b) markedly changes the relative binding energy shifts with applied voltage. The binding energies in the Ti 2p and Ni 2p data sets for this electrode are nearly constant with respect to applied potential, indicating that the band bending within the semiconductor does not markedly change across this potential range. This suggests that the TiO_2/Ni combination acts like a metal when in contact with the electrolyte. As this combination is also highly conductive, these results are consistent with the observed electrochemical behavior of the samples. These results are summarized in Figure 8; we believe this general approach to be appropriate for the investigation of various semiconductor/liquid combinations. Although the Ni film will contain a Ni/NiOx intermixed layer, the distinction here does not alter these conclusions substantially. A more rigorous analysis can be found in [27].

[Place Figure 7 here]
[Place Figure 8 here]

A further piece of information that can be extracted from the data collected is the flat-band potential U_{fb} for a semiconductor/liquid junction. For appropriately doped semiconductors the width of the space-charge region d_{scr} is on the order of a few photoelectron escape depths λ, i.e. $0.1<d_{scr}/3\lambda<10$. For this situation, the emitted photoelectrons originate from the band bending region of the electrode and their energy is modified by the course of the band bending with position relative to the outmost semiconductor surface. This rather small variation in energy with position in the semiconductor (band bendings are of the order of a few tenths to 1 electron volt) results in a broadening of the measured core level due to the superposition of the kinetic energies of electrons emitted elastically from different depths. Accordingly, the width of the semiconductor core level peak (here, Ti 2p) broadens with increasing band bending, and is smallest when the band bending is absent, i.e. at the flat-band potential. As a result, plotting the full-width at half-maximum (FWHM) should show a minimum at the flat-band potential. As shown in Figure 7c, this was the case for the representative data collected herein; Mott-Schottky analysis in Figure 6c confirmed that the observed flat-band potential at -0.9 V vs. Ag/AgCl was consistent with investigation by electrochemical methods.

Figure 1: Solid/liquid junction. Illustration showing the band diagram and charge carrier density for (a) flat-band, (b) accumulation, (c) depletion and (d) inversion of an n-type semiconductor/liquid junction with n_e the free electron concentration, n_h the free hole concentration and n_i the intrinsic carrier concentration. The width of space-charge region is show as an accumulation layer d_{acc}, a depletion layer d_{dep} or an inversion layer d_{inv}. For further discussion, see [29]. Abbreviations are as follows: CBM: Conduction Band Minimum; VBM: Valence Band Maximum; E_F: Fermi Energy; U: the applied potential with respect to flat band; U_{FB} the flat band potential; $\bar{\mu}_e^S$: the chemical potential in the solution as described in reference [23].

Figure 2: XPS Schematic. Illustration of the XPS method: (a) standard XPS geometry; (b) Simulated XPS spectra of TiO_2 with core levels (CL), Auger lines and work function measurement; (c) Energy band relations for TiO_2 and definitions of kinetic energies E_{Kvac}, binding energies E_B and work function ϕ.

Figure 3: *Operando* AP-XPS setup. (a) Scheme of the operando XPS setup. The working electrode and the hemispherical electron energy analyzer (HEA) were grounded together. The potential of the working electrode was changed with respect to the reference electrode. The PEC-beaker containing the electrolyte could be lowered whereas the three-electrode mount could be moved in all three directions. (b) View into the high-pressure analysis chamber. The X-ray beam enters through the window on the left, the three-electrode setup is on the top, the electrolyte beaker on the bottom, and the electron analyzer cone is in the center. (c) Three-electrode setup pulled up and in measurement position (compare to (a)). (d) Photo of the actual "tender" X-Ray *operando* AP-XPS analyzer and the analysis chamber that is directly connected to the analyzer. (e) The energy band relations of the p^+-$Si/TiO_2/H_2O$(l.)/H_2O(g.) system under applied potential *U*. The working electrode (Si) and analyzer are grounded. In the three-electrode configuration the Fermi energy is shifted by *U* with respect to the reference electrode. The definitions of kinetic energies E_{Kvac}, binding energies E_B, work function ϕ and the ionization energy of H_2O (g.) E_{IE} are given. For p^+-$Si/TiO_2/Ni/H_2O$(l.)/H_2O(g.) electrodes, a thin film of Ni/NiO_x would also be present at the solid/liquid interface, and would influence band bending as discussed in the text. For a further analysis of the importance of the Ni/NiO_x film, please see [27].

Figure 4: ALD. (a) Illustration of one full ALD cycle for the growth of TiO_2 on Si/SiO_2. (b) Pressure variation in the ALD reactor during one cycle with times of precursor, oxygen, and purging pulses.

Figure 5: *Operando* AP-XPS data acquisition. (a) Sample is dipped into the electrolyte, CVs are recorded and the potential *U* is set. (b) The sample is pulled up and placed in measurement position (while maintaining electrical contact of all three electrodes with the electrolyte). (c) Beam shutter is opened and the measurement spot is illuminated by X-rays. Sample position is corrected, if necessary, and core level spectra are recorded.

Figure 6: Core-level *Operando* AP-XPS data. (a) O 1s and Ti 2p core levels of the TiO_2/electrolyte electrode. (b) CV curve of the TiO_2/electrolyte electrode with arrows indicating the potentials at which XPS spectra were taken. (c) Mott-Schottky data for a p^+-Si/TiO_2 electrode, with U_{fb} calculated as -0.9 V vs. Ag/AgCl from a linear fit; a Randles circuit was used as the equivalent circuit. Data is from reference [18] and reproduced by permission of The Royal Society of Chemistry.

Figure 7: Relative Core-level Peak Shifts. Relative peak shifts with respect to the flat-band potential U_{fb} = -0.9 V vs. Ag/AgCl for the (a) p^+-Si/TiO_2 and (b) p^+-Si/TiO_2/Ni(60 s) electrode of the O 1s (H_2O), Ti 2p (TiO_2), and Ni (NiO_x) core levels. Also presented are full width at half maximum (FWHM) for the Ti $2p_{3/2}$ peak of the (c) p^+-Si/TiO_2 electrode and of the (d) p^+-Si/TiO_2/Ni(60 s) as a function of applied potential. Data is from reference [18] and reproduced by permission of The Royal Society of Chemistry.

Figure 8: Band diagram. Schematic energy diagram of the TiO_2/liquid junction. (a) For highly negative bias (U_1 region, red lines), band shifting in the TiO_2 is observed (< -1.2 V). (b) In the ideal semiconductor region U_2, from -0.9 V to -0.6 V (blue lines), band bending in the TiO_2 is observed with no further potential drop in the electrochemical double layer. (c) For increased positive biased (U_3 region, green lines), the Fermi level is pinned to the defect states, and the TiO_2 bands shift with the complete potential drop that occurs in the electrochemical double layer. (d) At potentials positive of -0.2 V (region U_4), ideal behavior is once again observed. In all cases, the shift in water O 1s binding energy is linear with the applied voltage. The Ti 2p binding energy shifts linearly for band bending regimes (U_2 and U_4) and remains constant for the band shifting regimes (U_1 and U_3). Data is from reference [18] and reproduced by permission of The Royal Society of Chemistry.

DISCUSSION:

The most critical steps in the technique for data collection are the application of voltage and the collection of the XPS data. The semiconductor preparation is necessarily crucial but can be generalized to any system where the semiconductor/liquid junction is stable enough to be investigated. However, for the choice of electrolyte, a number of experimental parameters must be considered. First, there must be sufficient interaction (hydrophilic or hydrophobic) between the solid electrode and the electrolyte in order to form a thin stable meniscus; hydrophilic samples will generally work with water while hydrophobic samples will more likely work with organic solvents. Further, the electrolyte must not precipitate while under vacuum or due to slight temperature changes, and must have negligible vapor pressure. Precipitates can clog the detection cone. Furthermore, the electrode must not corrode or undergo chemical reactions over the course of the experiments, unless the measurement of such corrosion or reactions is itself the goal of the work.

Because these experiments generally observe the relative changes in binding energies with varied potential as opposed to absolute values of binding energies, the calibration with a gold (or other metal) standard is not absolutely required. However, the absolute binding energy values are also useful as these are informative as to the relative band edge placements of a semiconductor with respect to the solution as well as the orientation of the band edges with respect to other energetic states in the solid of interest. Furthermore, this calibration allows for the collected results to more easily be compared to standard UHV-XPS, in which the calibration is generally carried out prior to any experimentation.

Problems arising within the technique may be generally divided as follows. First, the core level in question must have a sufficiently high intensity in order for data thereof to be collected; if this is not the case, the count rate for the core level might be below the noise level in the data collected. A small photoionization cross section for interaction between the photon beam and the core level in question would lead to such an issue. This can be easily addressed by choosing proper core levels after collecting a survey scan prior to the application of voltages to the system; generally, the core level peak that is most intense for an aluminum Kα – based XPS (standard laboratory instrument) can be easily investigated by this technique as well. Second, the kinetic energy of the photoelectrons should be as high as possible, i.e. their binding energy should be as low as possible. This ensures an IMFP that is high enough to allow probing the semiconductor

energy bands below the liquid layer. Third, a clogged photoelectron collection cone is a very common problem and one that is best addressed through prevention; careful movements of the electrodes and beaker setups, as well as slow and cautious approach of the electrodes to the cone, will minimize the amount of solution that might interact with the cone. Care must also be taken to prevent the application of any potential that would cause substantial bubble formation as this can also provide a substantial amount of volatized material which can clog the cone. A clogged cone will result in decreasing count rates which will eventually make data collection impossible and require removal and cleaning of the cone itself, which requires a substantial amount of time (~8 hours). Fourth, the meniscus thickness must ideally be controlled to provide data on both the electrolyte and the solid; however, we have observed that different potentials may result in a thickening or thinning of the solution meniscus. As a result, it may be necessary to vary the potential window for data collection in order to observe photoelectron signals from all the constituents under investigation while maintaining three-electrode contact. A sample that is not sufficiently hydrophilic to maintain a stable meniscus may be made hydrophilic by careful oxidation of the surface; this is best carried out prior to data collection.

This technique, while powerful, has some limitations. Semiconductor and metal stability is important (outside of intentional corrosion studies) and the electrolyte window is limited to non-volatile materials such as KOH whereas liquid additives such as HCl would not be permissible. The photoionization cross section decreases with increased photon energy and is relatively small for photon energies used in this experiment resulting in an increased data collection time. Another consideration that must be taken into account is the bandwidth of the incoming photon beam. Monochromators can provide a very high resolving power, with $E/\Delta E$ of over 10000, whereas here, $E/\Delta E$ = 3000-7200. While this provides reasonable spectral resolution in the lower photon energy range (as used in laboratory XPS) the resolution decreases with increased photon energy, e.g. significant peak broadening can be observed, and fine structures, e.g. the spin orbit split in Si 2p, are not as well resolved. This, however, is only relevant for investigations of systems with numerous energetically close XPS core level peaks. Despite these limitations, however, this technique has substantially more power than standard XPS to resolve chemical changes at solid/liquid interfaces, because standard XPS requires a transfer into the XPS instrument and the application of ultra-high vacuum, during which the electrochemical nature of the material can change substantially. The *operando* AP-XPS approach furthermore can directly determine the nature of band bending in a semiconductor across a wide potential range, which is not possible using standard XPS on a semiconductor/liquid junction.

Further work using this technique will be applied to a wide variety of systems in which electrolytes and semiconductors, relevant for photoelectrochemical energy research, will be investigated. Corrosion analysis may be done directly with this methodology as opposed to the use of *ex-situ* analysis. Other semiconductor systems, particularly those relevant to the field of solar energy conversion such as transition metal oxides or technologically advanced group III-V and II-VI semiconductors are exciting systems for *operando* AP-XPS analysis. In particular, the influence of catalyst deposition on semiconductor energetics may be characterized. Systems such as crystalline $SrTiO_3$, $BiVO_4$ or InP, GaAs and ZnO can be considered as model systems for such work.

In conclusion, *operando* AP-XPS investigations of semiconductor/liquid junctions allow for the

description of the energetics at the interface and the nature of the junction. The type and magnitude of the band bending, accumulation, depletion, and inversion can be characterized as well as Fermi-level pinning and other attributes. While we only present data for TiO_2 and TiO_2/Ni in KOH electrolyte here, this approach can work for any semiconductor/liquid system that is consistent with the requirements presented in the above discussion section.

ACKNOWLEDGMENTS:
This work was supported through the Office of Science of the U.S. Department of Energy (DOE) under award No. DE SC0004993 to the Joint Center for Artificial Photosynthesis, a DOE Energy Innovation Hub. The Advanced Light Source is supported by the Director, Office of Science, Office of Basic Energy Sciences, of the U.S. Department of Energy under Contract No. DE AC02 05CH11231. The authors thank Dr. Philip Ross for contributions to the conceptual development of the *operando* AP-XPS endstation and experimental design.

DISCLOSURES:
The authors have nothing to disclose.

REFERENCES:
1 Walter, M. G. *et al.* Solar Water Splitting Cells. *Chem. Rev.* **110** (11), 6446-6473, doi:10.1021/cr1002326 (2010).
2 Bard, A. J. Design of semiconductor photoelectrochemical systems for solar energy conversion. *J. Phys. Chem.* **86** (2), 172-177, doi:10.1021/j100391a008 (1982).
3 Gerischer, H. Electrochemical photo and solar cells principles and some experiments. *J. Electroanal. Chem. Interfacial Electrochem.* **58** (1), 263-274, doi:10.1016/S0022-0728(75)80359-7 (1975).
4 Heller, A., Chang, K. C. & Miller, B. Spectral Response and Efficiency Relations in Semiconductor Liquid Junction Solar Cells. *J. Electrochem. Soc.* **124** (5), 697-700, doi:10.1149/1.2133385 (1977).
5 Prasad, G. & Srivastava, O. N. The high-efficiency (17.1%) WSe_2 photo-electrochemical solar cell. *J. Phys. D: Ap. Phys.* **21** (6), 1028 (1988).
6 Tan, M. X. *et al.* in *Progress in Inorganic Chemistry* 21-144 (John Wiley & Sons, Inc., 2007).
7 Salmeron, M. & Schlögl, R. Ambient pressure photoelectron spectroscopy: A new tool for surface science and nanotechnology. *Surf. Sci. Rep* **63** (4), 169-199, doi:10.1016/j.surfrep.2008.01.001 (2008).
8 Turner, N. H. Surface analysis: x-ray photoelectron spectroscopy and Auger electron spectroscopy. *Anal. Chem.* **60** (12), 377R-387R, doi:10.1021/ac00163a024 (1988).
9 Powell, C. J. & Jablonski, A. Progress in quantitative surface analysis by X-ray photoelectron spectroscopy: Current status and perspectives. *J. Electron. Spectrosc. Relat. Phenom.* **178–179**, 331-346, doi:10.1016/j.elspec.2009.05.004 (2010).
10 Fadley, C. S. Atomic-level characterization of materials with core- and valence-level photoemission: basic phenomena and future directions. *Surf. Interface Anal.* **40** (13), 1579-1605, doi:10.1002/sia.2902 (2008).
11 Kolmakov, A. *et al.* Graphene oxide windows for in situ environmental cell photoelectron spectroscopy. *Nat. Nano* **6** (10), 651-657, doi:10.1038/nnano.2011.130 (2011).

12 Masuda, T. *et al.* X-ray photoelectron spectroscopy for electrochemical reactions in ordinary solvents. *Appl. Phys. Lett.* **103** (11), 111605, doi: 10.1063/1.4821180 (2013).
13 Kraus, J. *et al.* Photoelectron spectroscopy of wet and gaseous samples through graphene membranes. *Nanoscale* **6** (23), 14394-14403, doi:10.1039/c4nr03561e (2014).
14 Ogletree, D. F. *et al.* A differentially pumped electrostatic lens system for photoemission studies in the millibar range. *Rev. Sci. Instrum.* **73** (11), 3872-3877, doi:10.1063/1.1512336 (2002).
15 Klyushin, A. Y., Rocha, T. C. R., Havecker, M., Knop-Gericke, A. & Schlogl, R. A near ambient pressure XPS study of Au oxidation. *Phys. Chem. Chem. Phys.* **16** (17), 7881-7886, doi:10.1039/c4cp00308j (2014).
16 Lu, Y.-C. *et al.* In Situ Ambient Pressure X-ray Photoelectron Spectroscopy Studies of Lithium-Oxygen Redox Reactions. *Sci. Rep.* **2**, doi: 10.1038/srep00715 (2012).
17 Kaichev, V. V., Prosvirin, I. P. & Bukhtiyarov, V. I. XPS for in situ study of the mechanisms of heterogeneous catalytic reactions. *J. Struct. Chem.* **52** (1), 90-101, doi:10.1134/s0022476611070134 (2011).
18 Axnanda, S. *et al.* Using "Tender" X-ray Ambient Pressure X-Ray Photoelectron Spectroscopy as A Direct Probe of Solid-Liquid Interface. *Sci. Rep.* **5**, 9788, doi:10.1038/srep09788 (2015).
19 Hu, S. *et al.* Amorphous TiO2 coatings stabilize Si, GaAs, and GaP photoanodes for efficient water oxidation. *Science* **344** (6187), 1005-1009, doi:10.1126/science.1251428 (2014).
20 Lichterman, M. F. *et al.* Stabilization of n-cadmium telluride photoanodes for water oxidation to O_2(g) in aqueous alkaline electrolytes using amorphous TiO_2 films formed by atomic-layer deposition. *Energy Environ. Sci.* **7** (10), 3334-3337, doi:10.1039/c4ee01914h (2014).
21 McDowell, M. T. *et al.* Improved Stability of Polycrystalline Bismuth Vanadate Photoanodes by Use of Dual-Layer Thin TiO_2/Ni Coatings. *J. Phys. Chem. C* **118** (34), 19618-19624, doi:10.1021/jp506133y (2014).
22 Lichterman, M. F. *et al.* (Invited) Investigation of the Si/TiO_2/Electrolyte Interface Using Operando Tender X-ray Photoelectron Spectroscopy. *ECS Trans.* **66** (6), 97-103, doi:10.1149/06606.0097ecst (2015).
23 Lichterman, M. F. *et al.* Direct observation of the energetics at a semiconductor/liquid junction by operando X-ray photoelectron spectroscopy. *Energy Environ. Sci.* **8** (8), 2409-2416, doi:10.1039/C5EE01014D (2015).
24 Richter, M. H. *et al.* (Invited) Measurement of the Energy-Band Relations of Stabilized Si Photoanodes Using Operando Ambient Pressure X-ray Photoelectron Spectroscopy. *ECS Trans.* **66** (6), 105-113, doi:10.1149/06606.0105ecst (2015).
25 Zhang, N., Yang, M.-Q., Liu, S., Sun, Y. & Xu, Y.-J. Waltzing with the Versatile Platform of Graphene to Synthesize Composite Photocatalysts. *Chem. Rev.* **115** (18), 10307-10377, doi:10.1021/acs.chemrev.5b00267 (2015).
26 Liu, S., Tang, Z.-R., Sun, Y., Colmenares, J. C. & Xu, Y.-J. One-dimension-based spatially ordered architectures for solar energy conversion. *Chem. Soc. Rev.* **44** (15), 5053-5075, doi:10.1039/c4cs00408f (2015).
27 Lichterman, M. F. *et al.* An Electrochemical, Microtopographical and Ambient Pressure X-Ray Photoelectron Spectroscopic Investigation of Si/TiO2/Ni/Electrolyte Interfaces. *J. Electrochem. Soc.* **163** (2), H139-H146, doi:10.1149/2.0861602jes (2016).

28 Bard, A. J., Bocarsly, A. B., Fan, F. R. F., Walton, E. G. & Wrighton, M. S. The concept of Fermi level pinning at semiconductor/liquid junctions. Consequences for energy conversion efficiency and selection of useful solution redox couples in solar devices. *J. Am. Chem. Soc.* **102** (11), 3671-3677, doi:10.1021/ja00531a001 (1980).
29 Li, L., Salvador, P. A. & Rohrer, G. S. Photocatalysts with internal electric fields. *Nanoscale* **6** (1), 24-42, doi:10.1039/c3nr03998f (2014).

Figure 1

Click here to download Figure figure_01a.tif

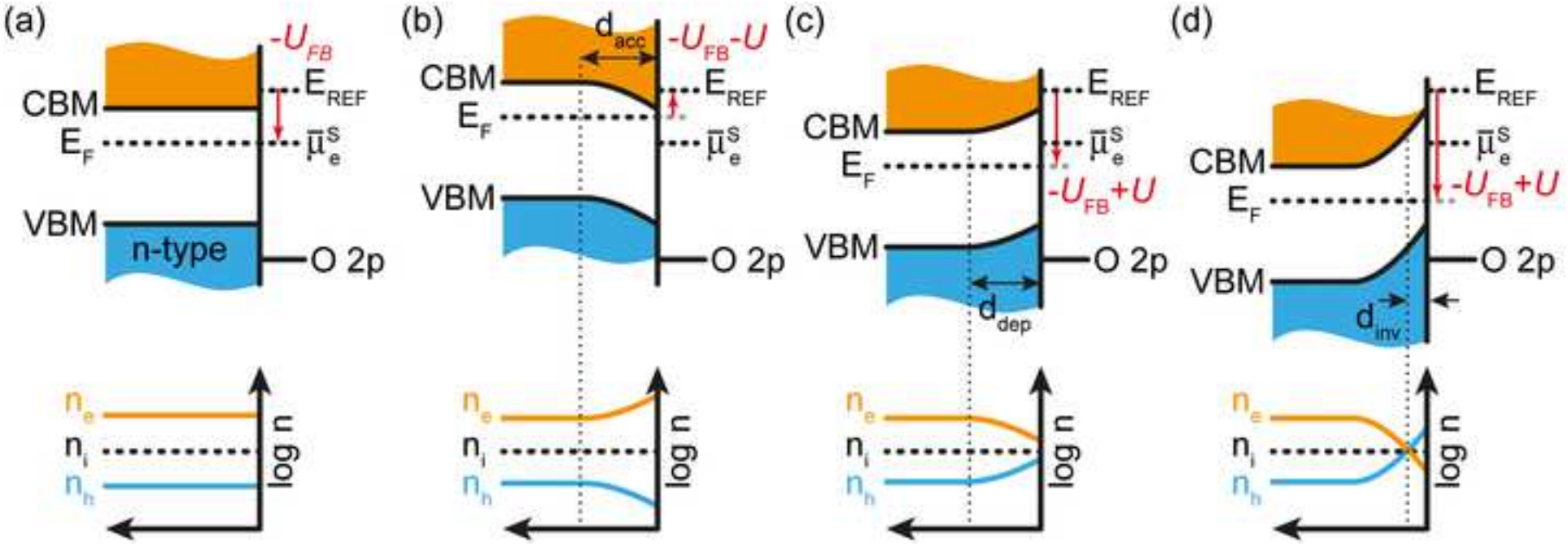

Figure 2

Click here to download Figure figure_02.tif

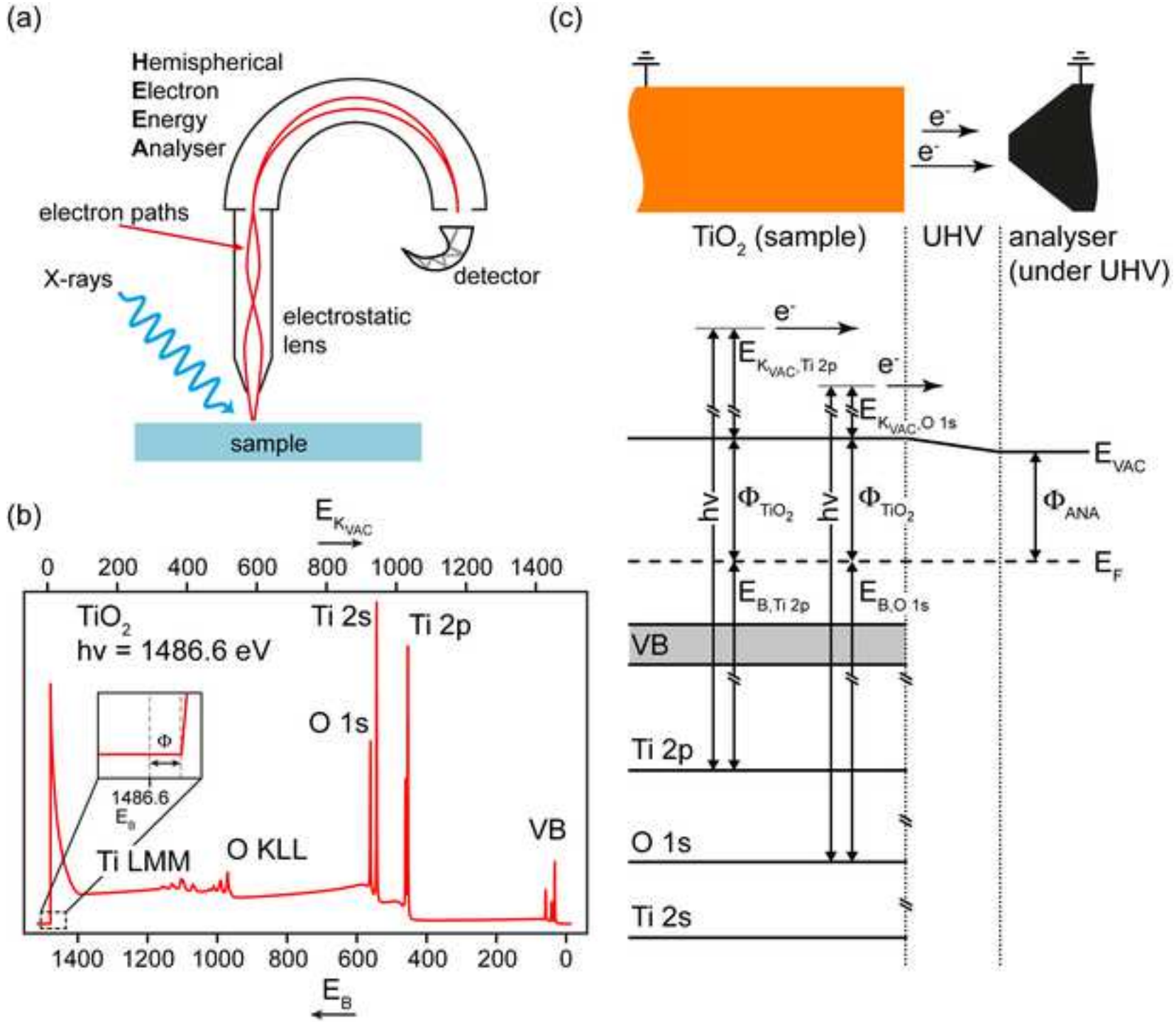

Figure 3

Click here to download Figure figure_03.tif

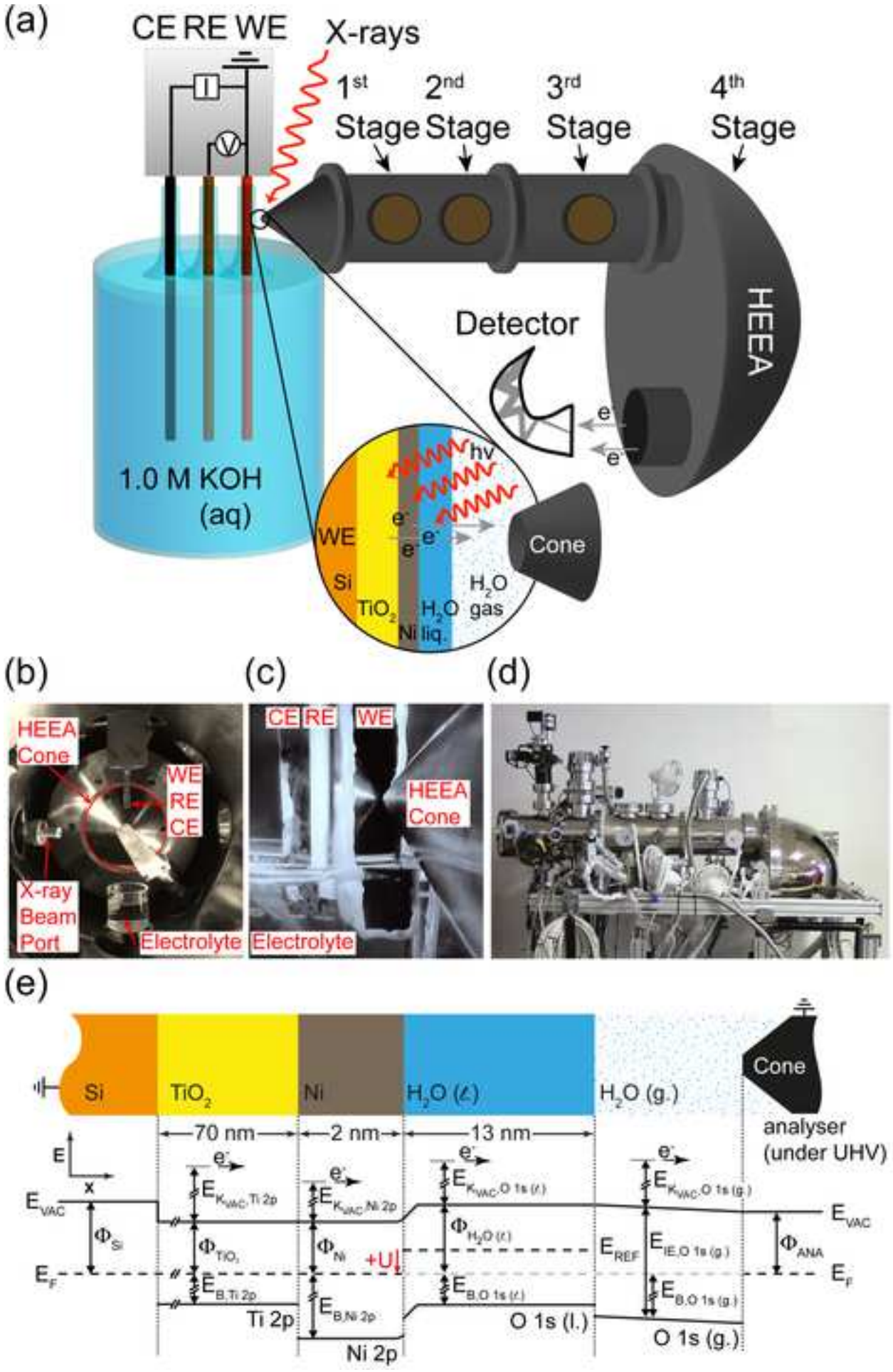

Figure 4

Click here to download Figure figure_04.tif

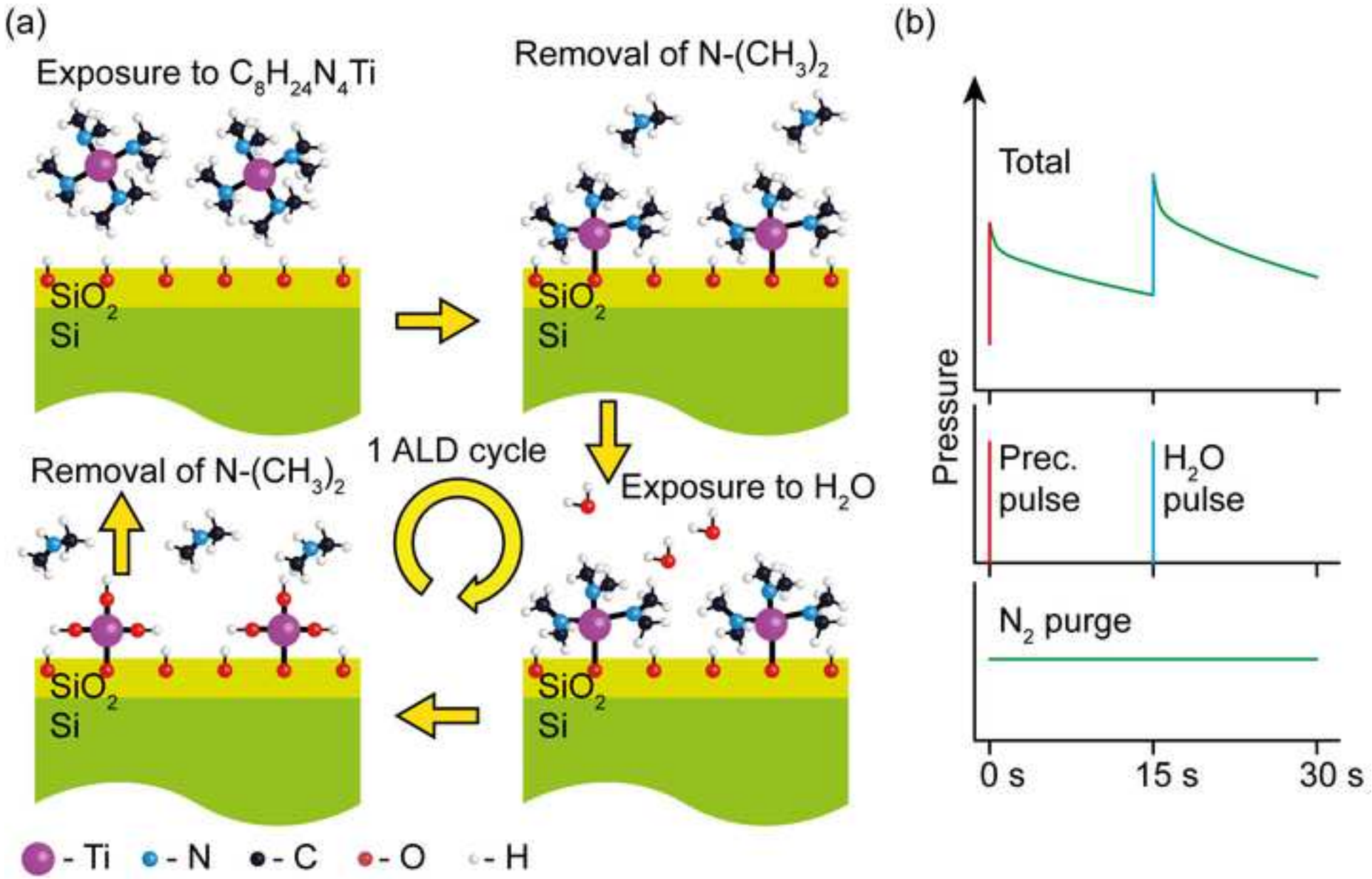

Figure 5

Click here to download Figure figure_05.tif

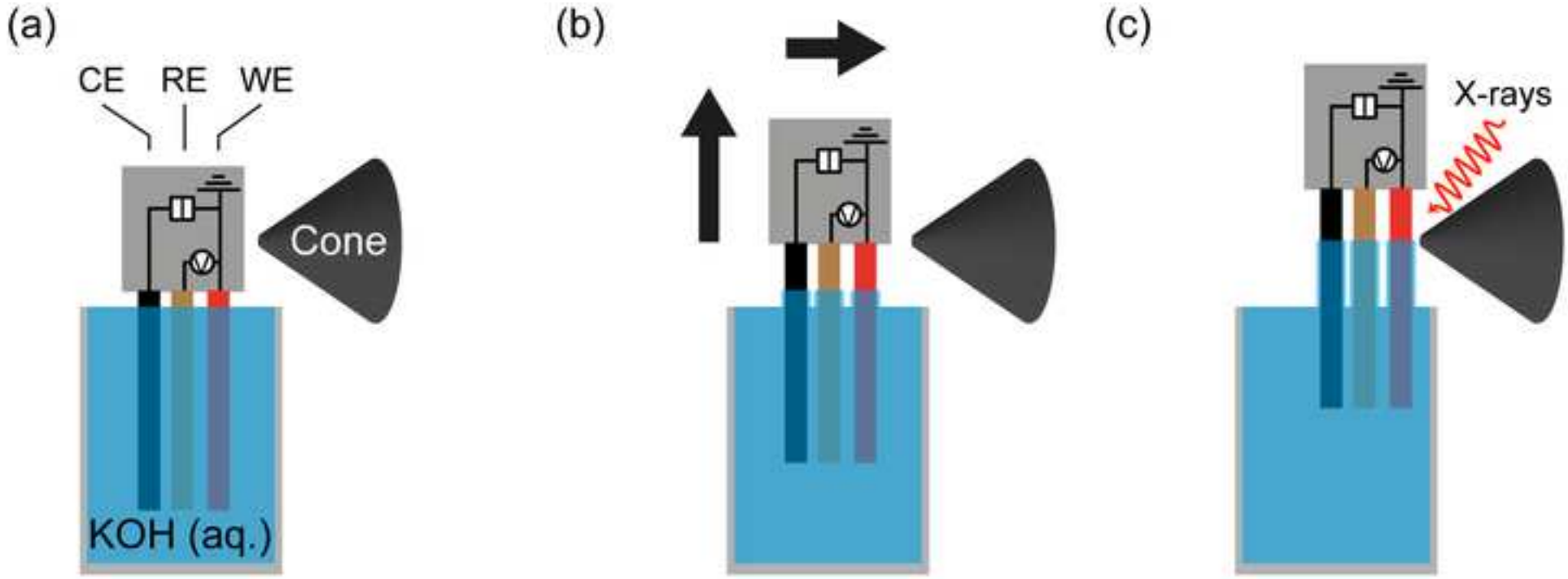

Figure 6

Click here to download Figure figure_06.tif

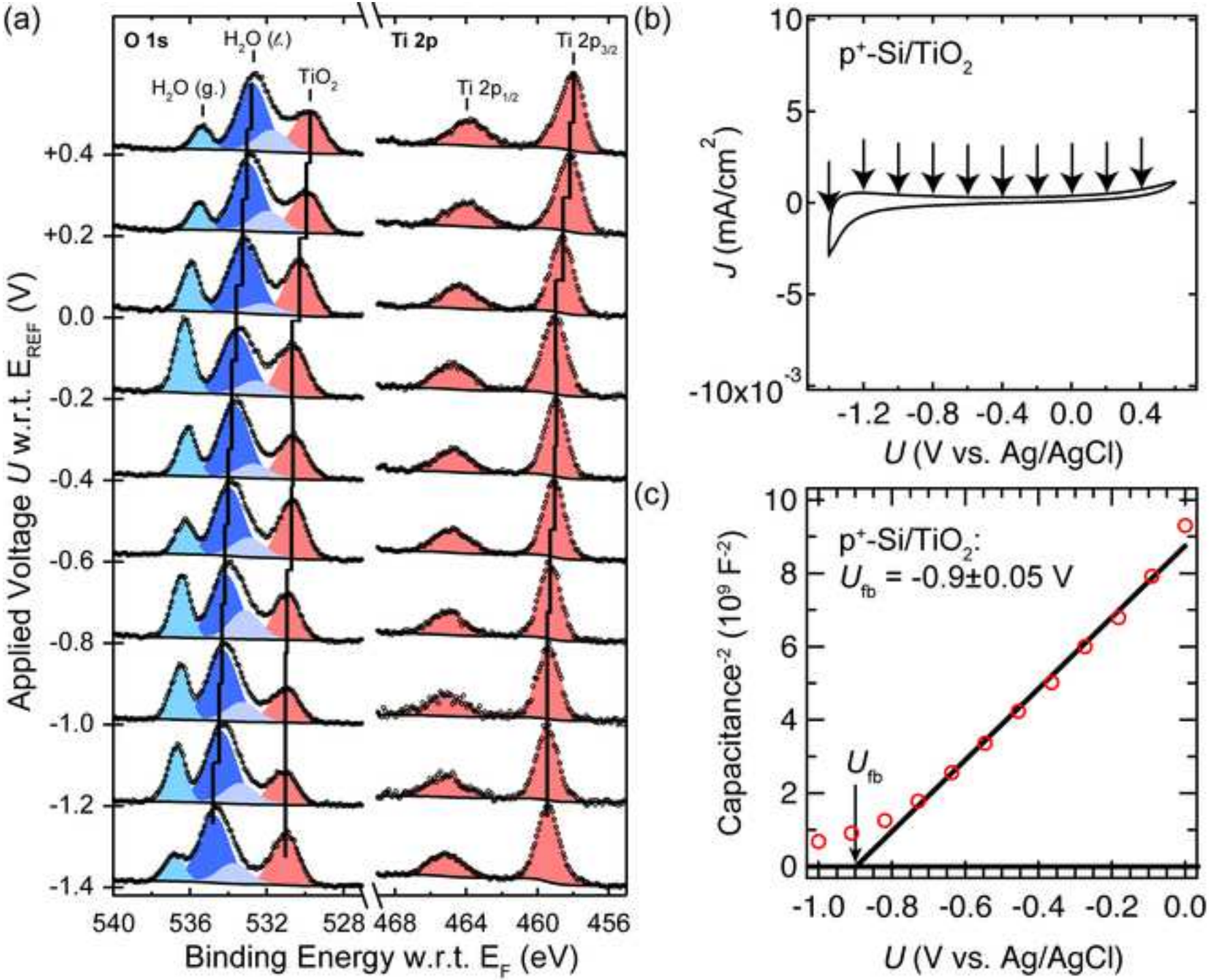

Figure 7

Click here to download Figure figure_07.tif

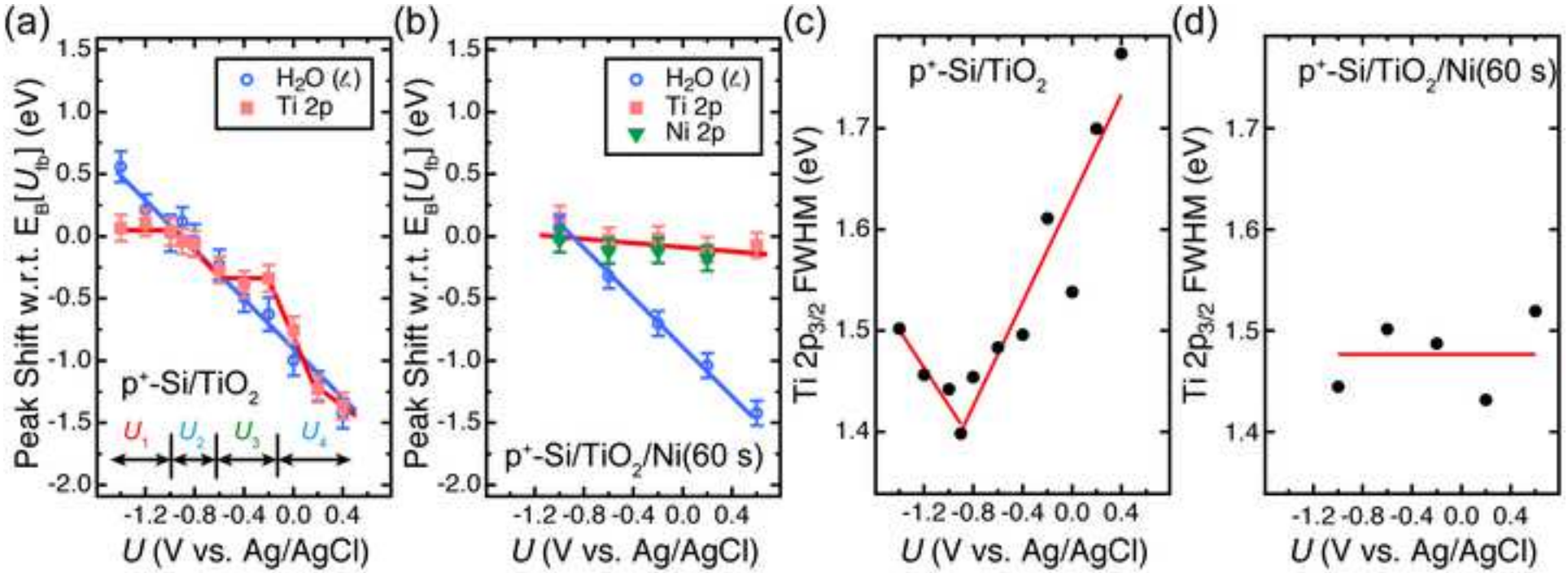

Figure 8

Click here to download Figure figure_08.tif

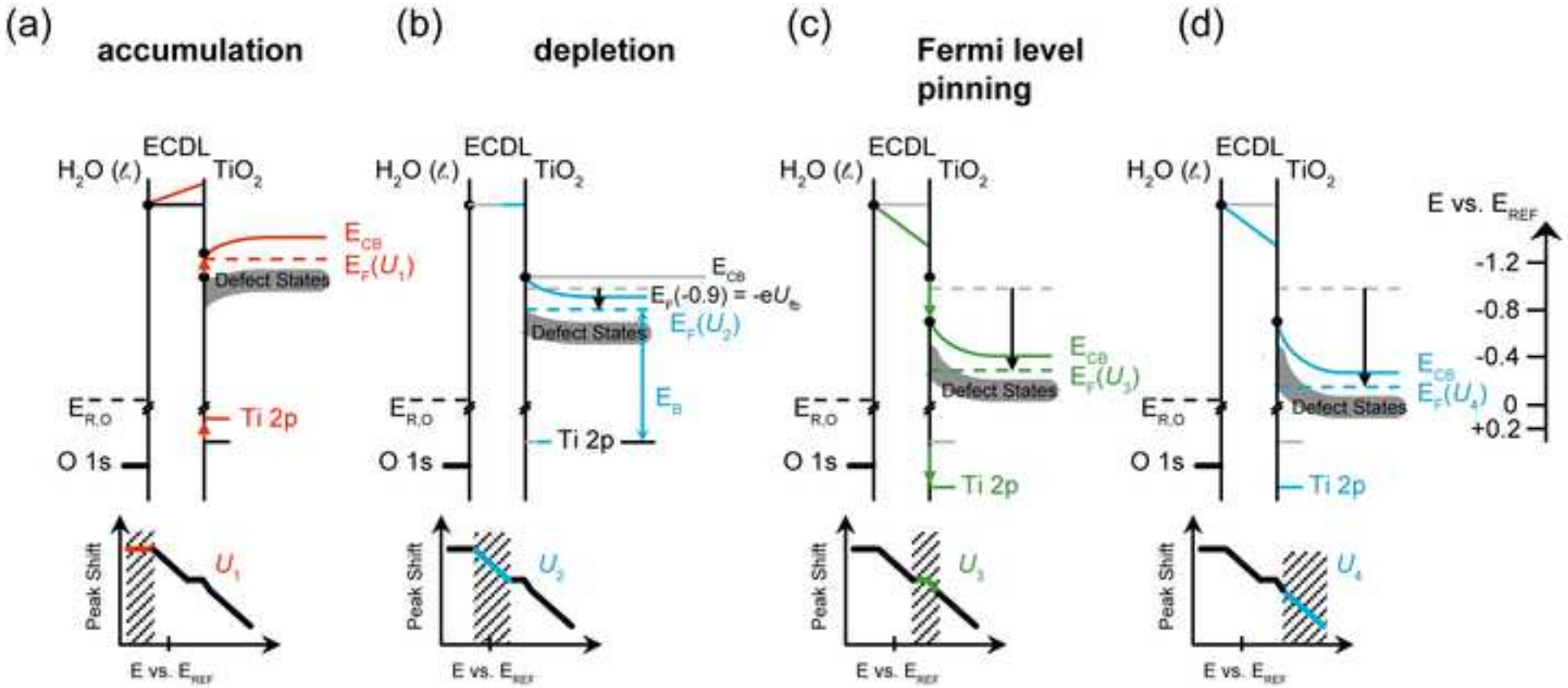

Excel Spreadsheet- Table of Materials/Equipment

Click here to download Excel Spreadsheet- Table of Materials/Equipment JoVE Materials spreadsheet_revised.xls

Name of Reagent/ Equipment	Company	Catalog Number
p^+-Si(100)	Addison	3P-111
H_2SO_4	Sigma Aldrich	339741
H_2O_2	Sigma Aldrich	216763
HF	Sigma Aldrich	339261
millipore H_2O	EMDMillipore	Milli-Q® Advantage A10
HCl	Sigma Aldrich	320331
Tetrakis(dimethylamido)titanium(IV) (TDMAT)	Sigma Aldrich	469858
N_2	Praxair	NI 6.0 RS
Ni target	AJA International	7440-02-0
In/Ga	Sigma Aldrich	495425
Hysol 9460	Ellsworth Adhesives	83128
KOH	Sigma Aldrich	306568
Liquid Nitrogen	Praxair	NI 5.0
Gold foil	Sigma Aldrich	326496
HNO_3	Sigma Aldrich	438073
1-sided copper tape	adafruit	1128
glass microscope slides	VWR	48300-025
Ag/AgCl reference electrode	eDaq	ET072-1
Platinum foil	Sigma Aldrich	349348
SP-300 Biologic Potentiostat	Biologic	SP-300
Scienta r4000 HiPP-2 Detector APPES	Scienta	HiPP-2

Comments/Description
Resistivity < 0.005 Ω - cm
99.999%
30%
99.99%
18.2 MΩ
ACS Reagent, 37%
99.999%
>99.9999%
>99.99%
>99.99%
Dual cartridge
Semiconductor grade, 99.99%
99.99%
ACS Reagent, 70%
For electrode construction
For electrode construction
99.99%

jove JOURNAL OF VISUALIZED EXPERIMENTS
1 Alewife Center #200
Cambridge, MA 02140
tel. 617.945.9051
www.jove.com

ARTICLE AND VIDEO LICENSE AGREEMENT

Title of Article: **Experimental Approach for Determining Semiconductor/liquid Junction Energetics by Operando AP-XPS Spectroscopy**

Author(s): **Michael F. Lichterman; Matthias H. Richter; Shu Hu; Ethan J. Crumlin; Stephanus Axnanda; Marco Favaro; Walter Drisdell; Zahid Hussain; Bruce S. Brunschwig; Nathan S. Lewis; Zhi Liu; Hans-Joachim Lewerenz**

Item 1 (check one box): The Author elects to have the Materials be made available (as described at http://www.jove.com/publish) via: ☑ Standard Access ☐ Open Access

Item 2 (check one box):

☑ The Author is NOT a United States government employee.

☐ The Author is a United States government employee and the Materials were prepared in the course of his or her duties as a United States government employee.

☐ The Author is a United States government employee but the Materials were NOT prepared in the course of his or her duties as a United States government employee.

ARTICLE AND VIDEO LICENSE AGREEMENT

1. Defined Terms. As used in this Article and Video License Agreement, the following terms shall have the following meanings: "**Agreement**" means this Article and Video License Agreement; "**Article**" means the article specified on the last page of this Agreement, including any associated materials such as texts, figures, tables, artwork, abstracts, or summaries contained therein; "**Author**" means the author who is a signatory to this Agreement; "**Collective Work**" means a work, such as a periodical issue, anthology or encyclopedia, in which the Materials in their entirety in unmodified form, along with a number of other contributions, constituting separate and independent works in themselves, are assembled into a collective whole; "**CRC License**" means the Creative Commons Attribution-Non Commercial-No Derivs 3.0 Unported Agreement, the terms and conditions of which can be found at: http://creativecommons.org/licenses/by-nc-nd/3.0/legalcode; "**Derivative Work**" means a work based upon the Materials or upon the Materials and other pre-existing works, such as a translation, musical arrangement, dramatization, fictionalization, motion picture version, sound recording, art reproduction, abridgment, condensation, or any other form in which the Materials may be recast, transformed, or adapted; "**Institution**" means the institution, listed on the last page of this Agreement, by which the Author was employed at the time of the creation of the Materials; "**JoVE**" means MyJove Corporation, a Massachusetts corporation and the publisher of *The Journal of Visualized Experiments;* "**Materials**" means the Article and / or the Video; "**Parties**" means the Author and JoVE; "**Video**" means any video(s) made by the Author, alone or in conjunction with any other parties, or by JoVE or its affiliates or agents, individually or in collaboration with the Author or any other parties, incorporating all or any portion of the Article, and in which the Author may or may not appear.

2. Background. The Author, who is the author of the Article, in order to ensure the dissemination and protection of the Article, desires to have the JoVE publish the Article and create and transmit videos based on the Article. In furtherance of such goals, the Parties desire to memorialize in this Agreement the respective rights of each Party in and to the Article and the Video.

3. Grant of Rights in Article. In consideration of JoVE agreeing to publish the Article, the Author hereby grants to JoVE, subject to **Sections 4** and **7** below, the exclusive, royalty-free, perpetual (for the full term of copyright in the Article, including any extensions thereto) license (a) to publish, reproduce, distribute, display and store the Article in all forms, formats and media whether now known or hereafter developed (including without limitation in print, digital and electronic form) throughout the world, (b) to translate the Article into other languages, create adaptations, summaries or extracts of the Article or other Derivative Works (including, without limitation, the Video) or Collective Works based on all or any portion of the Article and exercise all of the rights set forth in (a) above in such translations, adaptations, summaries, extracts, Derivative Works or Collective Works and (c) to license others to do any or all of the above. The foregoing rights may be exercised in all media and formats, whether now known or hereafter devised, and include the right to make such modifications as are technically necessary to exercise the rights in other media and formats. If the "Open Access" box has been checked in **Item 1** above, JoVE and the Author hereby grant to the public all such rights in the Article as provided in, but subject to all limitations and requirements set forth in, the CRC License.

jove JOURNAL OF VISUALIZED EXPERIMENTS
1 Alewife Center #200
Cambridge, MA 02140
tel. 617.945.9051
www.jove.com

4. Retention of Rights in Article. Notwithstanding the exclusive license granted to JoVE in **Section 3** above, the Author shall, with respect to the Article, retain the non-exclusive right to use all or part of the Article for the non-commercial purpose of giving lectures, presentations or teaching classes, and to post a copy of the Article on the Institution's website or the Author's personal website, in each case provided that a link to the Article on the JoVE website is provided and notice of JoVE's copyright in the Article is included. All non-copyright intellectual property rights in and to the Article, such as patent rights, shall remain with the Author.

5. Grant of Rights in Video – Standard Access. This **Section 5** applies if the "Standard Access" box has been checked in **Item 1** above or if no box has been checked in **Item 1** above. In consideration of JoVE agreeing to produce, display or otherwise assist with the Video, the Author hereby acknowledges and agrees that, Subject to **Section 7** below, JoVE is and shall be the sole and exclusive owner of all rights of any nature, including, without limitation, all copyrights, in and to the Video. To the extent that, by law, the Author is deemed, now or at any time in the future, to have any rights of any nature in or to the Video, the Author hereby disclaims all such rights and transfers all such rights to JoVE.

6. Grant of Rights in Video – Open Access. This **Section 6** applies only if the "Open Access" box has been checked in **Item 1** above. In consideration of JoVE agreeing to produce, display or otherwise assist with the Video, the Author hereby grants to JoVE, subject to **Section 7** below, the exclusive, royalty-free, perpetual (for the full term of copyright in the Article, including any extensions thereto) license (a) to publish, reproduce, distribute, display and store the Video in all forms, formats and media whether now known or hereafter developed (including without limitation in print, digital and electronic form) throughout the world, (b) to translate the Video into other languages, create adaptations, summaries or extracts of the Video or other Derivative Works or Collective Works based on all or any portion of the Video and exercise all of the rights set forth in (a) above in such translations, adaptations, summaries, extracts, Derivative Works or Collective Works and (c) to license others to do any or all of the above. The foregoing rights may be exercised in all media and formats, whether now known or hereafter devised, and include the right to make such modifications as are technically necessary to exercise the rights in other media and formats. For any Video to which this Section 6 is applicable, JoVE and the Author hereby grant to the public all such rights in the Video as provided in, but subject to all limitations and requirements set forth in, the CRC License.

7. Government Employees. If the Author is a United States government employee and the Article was prepared in the course of his or her duties as a United States government employee, as indicated in **Item 2** above, and any of the licenses or grants granted by the Author hereunder exceed the scope of the 17 U.S.C. 403, then the rights granted hereunder shall be limited to the maximum rights permitted under such statute. In such case, all provisions contained herein that are not in conflict with such statute shall remain in full force and effect, and all provisions contained herein that do so conflict shall be deemed to be amended so as to provide to JoVE the maximum rights permissible within such statute.

8. Likeness, Privacy, Personality. The Author hereby grants JoVE the right to use the Author's name, voice, likeness, picture, photograph, image, biography and performance in any way, commercial or otherwise, in connection with the Materials and the sale, promotion and distribution thereof. The Author hereby waives any and all rights he or she may have, relating to his or her appearance in the Video or otherwise relating to the Materials, under all applicable privacy, likeness, personality or similar laws.

9. Author Warranties. The Author represents and warrants that the Article is original, that it has not been published, that the copyright interest is owned by the Author (or, if more than one author is listed at the beginning of this Agreement, by such authors collectively) and has not been assigned, licensed, or otherwise transferred to any other party. The Author represents and warrants that the author(s) listed at the top of this Agreement are the only authors of the Materials. If more than one author is listed at the top of this Agreement and if any such author has not entered into a separate Article and Video License Agreement with JoVE relating to the Materials, the Author represents and warrants that the Author has been authorized by each of the other such authors to execute this Agreement on his or her behalf and to bind him or her with respect to the terms of this Agreement as if each of them had been a party hereto as an Author. The Author warrants that the use, reproduction, distribution, public or private performance or display, and/or modification of all or any portion of the Materials does not and will not violate, infringe and/or misappropriate the patent, trademark, intellectual property or other rights of any third party. The Author represents and warrants that it has and will continue to comply with all government, institutional and other regulations, including, without limitation all institutional, laboratory, hospital, ethical, human and animal treatment, privacy, and all other rules, regulations, laws, procedures or guidelines, applicable to the Materials, and that all research involving human and animal subjects has been approved by the Author's relevant institutional review board.

10. JoVE Discretion. If the Author requests the assistance of JoVE in producing the Video in the Author's facility, the Author shall ensure that the presence of JoVE employees, agents or independent contractors is in accordance with the relevant regulations of the Author's institution. If more than one author is listed at the beginning of this Agreement, JoVE may, in its sole discretion, elect not take any action with respect to the Article until such time as it has received complete, executed Article and Video License Agreements from each such author. JoVE reserves the right, in its absolute and sole discretion and without giving any reason therefore, to accept or decline any work submitted to JoVE. JoVE and its employees, agents and independent contractors shall have

jove JOURNAL OF VISUALIZED EXPERIMENTS
1 Alewife Center #200
Cambridge, MA 02140
tel. 617.945.9051
www.jove.com

ARTICLE AND VIDEO LICENSE AGREEMENT

full, unfettered access to the facilities of the Author or of the Author's institution as necessary to make the Video, whether actually published or not. JoVE has sole discretion as to the method of making and publishing the Materials, including, without limitation, to all decisions regarding editing, lighting, filming, timing of publication, if any, length, quality, content and the like.

11. Indemnification. The Author agrees to indemnify JoVE and/or its successors and assigns from and against any and all claims, costs, and expenses, including attorney's fees, arising out of any breach of any warranty or other representations contained herein. The Author further agrees to indemnify and hold harmless JoVE from and against any and all claims, costs, and expenses, including attorney's fees, resulting from the breach by the Author of any representation or warranty contained herein or from allegations or instances of violation of intellectual property rights, damage to the Author's or the Author's institution's facilities, fraud, libel, defamation, research, equipment, experiments, property damage, personal injury, violations of institutional, laboratory, hospital, ethical, human and animal treatment, privacy or other rules, regulations, laws, procedures or guidelines, liabilities and other losses or damages related in any way to the submission of work to JoVE, making of videos by JoVE, or publication in *JoVE* or elsewhere by JoVE. The Author shall be responsible for, and shall hold JoVE harmless from, damages caused by lack of sterilization, lack of cleanliness or by contamination due to the making of a video by JoVE its employees, agents or independent contractors. All sterilization, cleanliness or decontamination procedures shall be solely the responsibility of the Author and shall be undertaken at the Author's expense. All indemnifications provided herein shall include JoVE's attorney's fees and costs related to said losses or damages. Such indemnification and holding harmless shall include such losses or damages incurred by, or in connection with, acts or omissions of JoVE, its employees, agents or independent contractors.

12. Fees. To cover the cost incurred for publication, JoVE must receive payment before production and publication the Materials. Payment is due in 21 days of invoice. Should the Materials not be published due to an editorial or production decision, these funds will be returned to the Author. Withdrawal by the Author of any submitted Materials after final peer review approval will result in a US$1,200 fee to cover pre-production expenses incurred by JoVE. If payment is not received by the completion of filming, production and publication of the Materials will be suspended until payment is received.

13. Transfer, Governing Law. This Agreement may be assigned by JoVE and shall inure to the benefits of any of JoVE's successors and assignees. This Agreement shall be governed and construed by the internal laws of the Commonwealth of Massachusetts without giving effect to any conflict of law provision thereunder. This Agreement may be executed in counterparts, each of which shall be deemed an original, but all of which together shall be deemed to me one and the same agreement. A signed copy of this Agreement delivered by facsimile, e-mail or other means of electronic transmission shall be deemed to have the same legal effect as delivery of an original signed copy of this Agreement.

A signed copy of this document must be sent with all new submissions. Only one Agreement required per submission.

CORRESPONDING AUTHOR:

Name: Michael Lichterman

Department: Chemistry and Chemical Engineering

Institution: California Institute of Technology

Article Title: **Experimental Approach for Determining Semiconductor/liquid Junction Energetics by Operando AP-XPS Spectroscopy**

Signature: 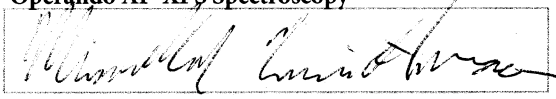 Date: Sept 15, 2015

Please submit a signed and dated copy of this license by one of the following three methods:

1) Upload a scanned copy of the document as a pfd on the JoVE submission site;
2) Fax the document to +1.866.381.2236;
3) Mail the document to JoVE / Attn: JoVE Editorial / 1 Alewife Center #200 / Cambridge, MA 02139

For questions, please email submissions@jove.com or call +1.617.945.9051

Click here to download Rebuttal Comments
JoVE_Third_responses.docx

1. Please take this opportunity to thoroughly proofread the manuscript to ensure that there are no spelling or grammar issues. The JoVE editor will not copy-edit your manuscript and any errors in the submitted revision may be present in the published version.

Author Response: Various slight changes to wording and formatting have been carried out for clarity and consistency.

2. Please add more explicit details. For software steps, we need explicit step-wise instructions if a step is to be filmed: File | Save | etc.
For steps 4.5/4.6, what is done to collect the XPS data? What are the collection parameters? How many frames? etc. What is clicked on to start the process?
For steps 5.5-5.7, what is done to collect the data? What are the collection parameters? etc.

Author Response: As these are essentially identical, a description is added to step 5.6; in step 4.6, a note is added to direct the reader to the description in step 5.6. The text is as follows: “Generally, this consists of opening the scan selection window within the software by selecting “setup” from the “run” pull-down menu. On the setup page, selecting a scan and clicking “edit” will allow the user to modify the energy parameters of the scan; alternately, a new scan profile, by selecting “new,” can be entered. Selecting a “check mark” next to a scan will select the scan to be carried out, and clicking “start” will start the acquisition.”

Click here to access/download
Supplemental File (as requested by JoVE)
Jove_Permissions.docx